

Organization of the Synaptonemal Complex During Meiosis in *Caenorhabditis elegans*

Kristina Schild-Prüfert,^{*,1} Takamune T. Saito,^{*,2} Sarit Smolikov,^{*,2,3} Yanjie Gu,^{*,2} Marina Hincapie,^{*,4}

David E. Hill,^{*,†} Marc Vidal,^{*,†} Kent McDonald,[‡] and Monica P. Colaiácovo^{*,5}

^{*}Department of Genetics, Harvard Medical School, Boston, Massachusetts 02115, [†]Center for Cancer Systems Biology (CCSB) and Department of Cancer Biology, Dana-Farber Cancer Institute, Boston, Massachusetts 02115, and [‡]Electron Microscope Laboratory, University of California, Berkeley, California 94720

ABSTRACT Four different SYP proteins (SYP-1, SYP-2, SYP-3, and SYP-4) have been proposed to form the central region of the synaptonemal complex (SC) thereby bridging the axes of paired meiotic chromosomes in *Caenorhabditis elegans*. Their interdependent localization suggests that they may interact within the SC. Our studies reveal for the first time how these SYP proteins are organized in the central region of the SC. Yeast two-hybrid and co-immunoprecipitation studies show that SYP-1 is the only SYP protein that is capable of homotypic interactions, and is able to interact with both SYP-2 and SYP-3 directly, whereas SYP-2 and SYP-3 do not seem to interact with each other. Specifically, the coiled-coil domain of SYP-1 is required both for its homotypic interactions and its interaction with the C-terminal domain of SYP-2. Meanwhile, SYP-3 interacts with the C-terminal end of SYP-1 via its N-terminal domain. Immunoelectron microscopy analysis provides insight into the orientation of these proteins within the SC. While the C-terminal domain of SYP-3 localizes in close proximity to the chromosome axes, the N-terminal domains of both SYP-1 and SYP-4, as well as the C-terminal domain of SYP-2, are located in the middle of the SC. Taking into account the different sizes of these proteins, their interaction abilities, and their orientation within the SC, we propose a model of how the SYP proteins link the homologous axes to provide the conserved structure and width of the SC in *C. elegans*.

THE meiotic cell division process is unique in that it reduces the number of chromosomes by half, resulting in the formation of haploid gametes. This reduction in chromosome number is accomplished by following a single round of DNA replication with two consecutive rounds of meiotic chromosome segregation. During meiosis I (the reductional division), homologs segregate away from each other, while during meiosis II (the equational division), sister chromatids are separated. To successfully achieve the formation of haploid gametes, chromosomes undergo homologous pairing,

synapsis, and recombination during meiosis I. Problems in any of these processes can result in chromosome missegregation and the formation of aneuploid gametes, underscoring the importance of meiosis for sexually reproducing organisms and obtaining genetic diversity (Zickler and Kleckner 1999; Page and Hawley 2003).

Of particular importance during meiosis is the formation of a proteinaceous structure known as the synaptonemal complex (SC), which assembles at the interface between homologs, thereby stabilizing pairing interactions and promoting the completion of crossover recombination events (reciprocal exchanges of genetic information) between homologs (Page and Hawley 2004). The SC is a tripartite structure ubiquitously present from yeast to humans (Zickler and Kleckner 1999). First, proteins associate along chromosome axes forming the axial elements, which are referred to as lateral elements in the context of the fully formed SC. As the axes of homologous chromosomes align, central region components of the SC, consisting of transverse filament proteins, and in many cases also a central element, bridge the gap between lateral elements, thereby connecting the

Copyright © 2011 by the Genetics Society of America

doi: 10.1534/genetics.111.132431

Manuscript received May 9, 2011; accepted for publication July 25, 2011

Supporting information is available online at <http://www.genetics.org/content/suppl/2011/08/12/genetics.111.132431.DC1>.

¹Present address: Department of Microbiology, Institute of Molecular Biosciences, University of Graz, Graz 8010, Austria.

²These authors contributed equally to this work.

³Present address: Department of Biology, University of Iowa, Iowa-City, IA 52242.

⁴Present address: Barnett Institute and Department of Chemistry and Chemical Biology, Northeastern University, Boston, MA 02115.

⁵Corresponding author: Harvard Medical School, Department of Genetics, 77 Avenue Louis Pasteur, NRB-334, Boston, MA 02115.

E-mail: mcolaiacovo@genetics.med.harvard.edu

homologs (Page and Hawley 2004). Although this meiotic structure is present in most sexually reproducing organisms, SC formation and organization are still poorly understood.

A number of structural components of the SC have been identified in different organisms. Interestingly, while some degree of homology is shared among lateral element proteins throughout different organisms, central region components lack such homology. Specifically, Zip1 in *Saccharomyces cerevisiae* (Sym *et al.* 1993), C(3)G in *Drosophila melanogaster* (Page and Hawley 2001), ZYP1 in *Arabidopsis thaliana* (Higgins *et al.* 2005; Osman *et al.* 2006), SYP-1, SYP-2, SYP-3, and SYP-4 in *Caenorhabditis elegans* (MacQueen *et al.* 2002; Colaiacovo *et al.* 2003; Smolikov *et al.* 2007, 2009), and SCP1 in mammals (Meuwissen *et al.* 1992), share only a similar secondary structure consisting of a central coiled-coil domain flanked by globular N- and C-terminal domains (Hunter 2003). Many of these proteins form the transverse filaments responsible in part for the zipper-like organization that is characteristic of the SC. In recent years, additional proteins were identified as acting in the central region of the SC in both mammals and *Drosophila*. The *Drosophila* CONA (Page *et al.* 2008) and the mammalian SYCE1, SYCE2, SYCE3, and TEX12 proteins (Costa *et al.* 2005; Hamer *et al.* 2006; Bolcun-Filas *et al.* 2007; Page *et al.* 2008; Schramm *et al.* 2011) are proposed to bind either directly or indirectly to the transverse filaments, possibly stabilizing the zipper-like structure of the SC.

Whereas immunofluorescence analysis revealed that transverse filament proteins are found at the interface between homologous chromosomes, electron microscopy studies have been addressing their organization within this region. Studies in yeast demonstrated that Zip1 is not only found in the central region of the SC, but that when overexpressed, it can also form aggregates corresponding to higher-order protein structures referred to as polycomplexes (Sym and Roeder 1995). This ability to acquire a higher-order structural organization was also detected for SCP1 (Liu *et al.* 1996) and C(3)G (Anderson *et al.* 2005; Jeffress *et al.* 2007). Several common features are observed in the process resulting in SC assembly in various systems. Namely, the transverse filament proteins first form polarized homodimers, which are later able to form polydimers. Moreover, while their C termini are anchored to chromosome axes their N termini can be found at the middle of the central region (Liu *et al.* 1996; Dong and Roeder 2000; Anderson *et al.* 2005). This arrangement is responsible for the distinctive and unique ladder-like organization that can be observed on electron microscopic images of the SC in various model organisms. Further support for an organization in which transverse filament proteins lie perpendicular to the chromosome axes stems from observations that the distance between the lateral elements greatly depends on the length of the coiled-coil domain present in the transverse filament components. Specifically, studies in yeast demonstrated that the width of the SC is increased in a manner that is proportional to the increase in the length of the coiled-coil domain of the Zip1 protein (Sym and Roeder 1995). Similar results were

found for SCP1, which was overexpressed in a heterologous system and mimics this SC-like structure by forming polycomplexes, which vary in width if the expressed SCP1 carries deletions (Öllinger *et al.* 2005). Therefore, it is even more striking that these proteins, which not only differ in size and primary amino acid sequence, but also in numbers throughout organisms, are responsible for creating an SC that exhibits a conserved width of ~100 nm in most systems (Goldstein 1987; Sym *et al.* 1993; Zickler and Kleckner 1999; Page and Hawley 2003).

C. elegans offers a unique scenario in which to further investigate SC organization. It is a multicellular organism in which various of the key events of meiosis are conserved and in which multiple central region components have now been identified. Immunolocalization revealed that the four central region components of the *C. elegans* SC localize at the interface between homologous chromosomes during the pachytene stage of meiosis, when the SC is fully formed (MacQueen *et al.* 2002; Colaiacovo *et al.* 2003; Smolikov *et al.* 2007, 2009). Recent measurements of wild-type *C. elegans* SCs confirmed that the average width of the SC is approximately 100 nm (Smolikov *et al.* 2008). Furthermore, the loss of any one of these proteins impairs the chromosomal localization of the other three proteins, and as a result, SC formation is abrogated (Colaiacovo *et al.* 2003; Smolikov *et al.* 2007, 2009).

In this article we address the issue of how the SYP proteins interact with each other and are organized to establish the SC structure in *C. elegans*. We examined the interactions of SYP-1, SYP-2, SYP-3, and SYP-4 by two independent methods: (1) a yeast two-hybrid analysis and (2) co-immunoprecipitations studies. These studies revealed that SYP-1 can undergo homotypic interactions using its coiled-coil domain, and also interacts with SYP-2 and SYP-3. The interaction of SYP-1 with SYP-2 requires both the coiled-coil domain of SYP-1 and the C-terminal domain of SYP-2. We also show that SYP-1 interacts with SYP-3 via the N-terminal region of SYP-3 and the C-terminal region of SYP-1. The observation that SYP-1 interacts with both SYP-2 and SYP-3 provides a link between what had been previously thought of as two separate structural modules within the SC (SYP-1/SYP-2 and SYP-3/SYP-4). Finally, to examine the organization of the SYP proteins, immunoelectron microscopy was successfully implemented for the first time in studies of meiotic macromolecular structures in *C. elegans*. Using antibodies recognizing either the N or C termini of all four SYP proteins, we assessed how these proteins are distributed with regard to each other and the chromosome axes within the SC. These studies lead us to propose a model of how these central region components interact to form the SC in *C. elegans*, suggesting an organization that closely resembles that observed in mammals.

Materials and Methods

Strains

C. elegans strains were cultured at 20° under standard conditions (Brenner 1974). Bristol N2 worms were utilized as

the wild-type background. The following mutations and chromosome rearrangements were used (MacQueen *et al.* 2002; Colaiacovo *et al.* 2003; Smolikov *et al.* 2007, 2009):

LG I: *syp-3(me42, ok758)*, *syp-4(tm2713)*, *hT2[bli-4(e937) qIs48]* (I;III)

LG IV: *nT1[unc-?(n754) let-?(m435)]* (IV; V)

LG V: *syp-2(ok307)*, *syp-1(me17)*

DAPI analysis and immunostaining

Gonads were dissected from age-matched hermaphrodites 24 hr post-L4. DAPI staining, immunostaining, and analysis of stained meiotic nuclei were carried out as in Colaiacovo *et al.* (2003). The following primary antibodies were utilized at a 1:100 dilution: guinea pig α -SYP-1, rabbit α -SYP-2, rabbit α -SYP-3, and rabbit α -SYP-4. The secondary antibodies utilized were: Cy3 anti-rabbit and FITC anti-guinea-pig (Jackson Immunochemicals), each at 1:200.

Images were collected with an Olympus IX-70 microscope coupled to a cooled CCD camera (model CH350, Roper Scientific) driven by the DeltaVision system with SoftWorx software (Applied Precision). Data stacks consisted of 25–30 optical sections collected at 0.2- μ m increments. Images are projections halfway through 3D data stacks of whole nuclei.

Yeast two-hybrid protein-interaction assay

We utilized the Gateway cloning system (Invitrogen) to generate sequence-verified full-length and truncated *syp-1*, *syp-2*, and *syp-3* expression clones as in Boxem *et al.* (2008). First, the full-length predicted open reading frames (ORFs), as well as truncations consisting of removing either the N terminus (first 47, 97, and 60 amino acids for SYP-1, SYP-2, and SYP-3, respectively) or the C terminus (last 87, 52, and 44 amino acids for SYP-1, SYP-2, and SYP-3, respectively) for each of these genes, were PCR amplified from a mixed-stage *C. elegans* cDNA library and cloned into a Gateway compatible entry vector (pDONR223). Next, we utilized the full-length entry clones and forward and reverse primers designed at distance intervals of \sim 100 bp across each ORF, to generate a series of unbiased truncations (defined as unbiased for disregarding any specific protein domain) stemming from all possible primer combinations for each of our genes of interest. The resulting PCR fragments (ranging in size from 100 to 1370 bp, 542 bp, and 575 bp, respectively for *syp-1*, *syp-2*, and *syp-3*) were also cloned into pDONR223. Subsequently, full-length and truncated sequences were transferred into pDB-Amp (pDEST32) and pAD-Amp (pDEST22) destination vectors in a Gateway LR reaction.

Pairwise interactions between all proteins of interest (a total of 936 interactions) were examined in budding yeast cells by using Gal4 DNA binding domain (DB) and activation domain (AD) fusions, which were cotransformed into the yeast strain MaV103 described in Vidal *et al.* (1996). The yeast two-hybrid assay was performed as previously de-

scribed in Walhout and Vidal (2001) except that strains utilized for the β -galactosidase reporter assay were grown for 48 hr in liquid synthetic complete medium (SC) lacking tryptophan and leucine (-Trp, -Leu) and 3 μ l drops were spotted onto YEPD plates. These plates were then incubated at 30° for 48 hr before replica plating them onto YEPD plates containing nitrocellulose filters. Interactions were tested by scoring for activation of the *GAL1::lacZ* reporter gene after incubating the strains overnight at 37°. A subset of interactions, including all positive interactions detected using the β -galactosidase reporter assay described above, were then retested by assaying for growth on selective plates (SC–Leu–Trp–Ade). To this end, each entry clone was subcloned into 2 μ Gateway destination vectors pDB-Amp (pVV212) and pAD-Amp (pVV213) in a LR reaction. AD-Y and DB-X fusions were transformed into *MATa* Y8800 and *MAT α* Y8930 yeast strains, respectively. These yeast strains have three reporter genes: *GAL2-ADE2*, *met2::GAL7-lacZ*, and *LYS2::GAL1-HIS3*. *MATa* Y8800 and *MAT α* Y8930 were mated on YPD plates and diploids carrying both plasmids were selected on SC–Leu–Trp plates. Each transformant was cultured overnight in 200 μ l of liquid SC–Leu–Trp. Three-microliter drops were spotted onto SC–Leu–Trp and SC–Leu–Trp–Ade plates and incubated at 30° for 5 days. Primers used to generate clones examined in the yeast two-hybrid analysis in Figure 3 are described in Supporting Information, Table S1. Standard controls indicating no interaction (DB and AD without any fusion), a weak interaction (DB-pRB and AD-E2F1), and strong interactions (DB-Fos and AD-Jun; DB-Gal4p and AD; DB-DP and AD-E2F1; DB-DP and AD-CYH-E2F1) were used as described in Walhout and Vidal (2001).

Worm lysate and co-immunoprecipitation reactions

Worm lysates were prepared from adult worms grown on 20 100 \times 15-mm plates to a confluence of 70–80%, washed three times with M9 medium, and centrifuged at 3000 rpm for 15 min. The worm pellet was frozen in liquid nitrogen, resuspended with 5 \times volume of homogenization buffer (25 mM HEPES at pH 7.6, 5 mM EDTA, 0.5 M sucrose, 0.5% Chaps, 0.5% DOC) supplemented with complete protease inhibitor cocktail (Roche) and incubated in ice for 30 min. The solution was then sonicated three times for 1 min each and centrifuged at 3000 rpm for 15 min. The supernatant was removed and the procedure repeated two to three times. All supernatants were saved and tested on Western blots to confirm that both SYP-1 and SYP-2 could be detected in the worm lysate. A comparable analysis for SYP-3 and SYP-4 was not possible, given that our antibodies do not detect SYP-3 or SYP-4 on Western blots.

Immunoprecipitation was performed with protein A agarose beads (Roche). The beads were equilibrated with cold homogenization buffer (see above). To pre-clear about 200–300 μ g of worm lysate, the lysate was incubated with 25 μ l of equilibrated protein A beads at 4° for 1 hr. After removing the beads by centrifugation at 10000 \times g at 4° for 5 min, the lysate was transferred to a fresh tube and

incubated with 1 µg of affinity purified α -SYP-1 or α -SYP-2 antibody at 4° for 1 hr. Fresh equilibrated protein A beads, 25 µg, were then added to the solution and incubated overnight at 4°. Immunocomplexes bound to protein A beads were washed three times with cold homogenization buffer. After removing the supernatant, the proteins were eluted in 50 µl of Laemmli sample buffer (Laemmli 1970) by boiling for 10 min. The eluted proteins were separated from the beads by centrifugation at 14000 rpm at room temperature for 5 min and then transferred the supernatant to new tubes. Ten microliters was loaded in every lane for analysis on SDS-PAGE and immunoblotting using chemiluminescent detection (ECL, Pharmacia).

To identify putative interaction partners of SYP-3 and SYP-4 we set out to generate SYP-3 and SYP-4 GST and His tag fusion constructs for pull-down experiments and subsequent Western blot analysis. While the SYP-4 constructs proved difficult to express and purify under various conditions, we succeeded in performing these pull-down experiments with a SYP-3-GST fusion construct. However, an interaction between SYP-3 and either SYP-1 or SYP-2 was not observed by Western blot analysis of the SYP-3-GST pull-down probed with SYP-1 or SYP-2 specific antibodies (data not shown).

Immunoelectron microscopy

Wild-type adult hermaphrodites (24–26 hr post-L4) were prepared for electron microscopy by high-pressure freezing (HPF) followed by freeze substitution (McDonald 1998). For HPF, 15–20 worms were transferred to a specimen carrier (Leica, 1.5 × 0.2 mm) filled with bacteria and cryofixed in a high-pressure freezer (Leica EM PACT2/RTS). Frozen worms were kept in liquid nitrogen for at least 2 days before freeze substitution in 0.2% glutaraldehyde and 0.1% uranylacetate in acetone using the Leica automatic freeze-substitution system EM ATS2. The system was programmed for 2 hr at –92°, then warmed to –25° over a 13-hr period (slope 5), maintained for 5 hr at –25°, and then warmed to 0° over a 12-hr period (slope 2). Infiltration with LR-White (LRW) was utilized according to the following schedule: 3 × 5 min in 100% acetone, 3 × 5 min 50% acetone/ethanol, 3 × 5 min 100% ethanol. Followed by 30 min each in 25%, 50%, and 75% LRW in ethanol and finally in 100% LRW overnight. Worms were separated and mounted individually in flat-bottom capsules (Ted Pella) in LRW, which polymerized overnight at 68°.

Longitudinal 70-nm sections were cut on a Reichert Ultracut E ultramicrotome and picked up on Formvar/carbon-coated slot grids. Wild-type worms were immunolabeled with specific antibodies against SYP-1, SYP-2, SYP-3, SYP-4, and HTP-3 according to the following protocol: 15 min 0.4% glycine in PBS, 30 min in blocking buffer (BB; 0.8% BSA, 0.1% gelatin from cold water fish, Sigma, 0.002% Tween in PBS), 1 hr primary antibody in BB, 2 min in PBS/0.1% Tween, 4 × 3 min in BB, 1-hr secondary antibody in BB, 2 min in PBS/0.1% Tween, 6 × 3 min PBS, 5 min

in 0.5% glutaraldehyde in PBS, followed by a thorough wash with dH₂O. Samples were then post-stained with 4% uranylacetate in dH₂O and Reynolds lead for 7 min each with a thorough wash with dH₂O in between.

The primary antibodies utilized were guinea pig α -SYP-1 (N terminal) (MacQueen *et al.* 2002), rabbit α -SYP-2 (C terminal) (Colaiacovo *et al.* 2003), rabbit α -SYP-3 (C terminal) (Smolikov *et al.*, 2007), rabbit α -SYP-4 antibody (N terminal) (Smolikov *et al.* 2009) and guinea pig α -HTP-3 (Goodyer *et al.* 2008) each at 1:100. Secondary antibodies were coupled to either 15-nm gold (goat anti-guinea pig IgG (H+L); Ted Pella) or 10-nm gold (goat anti-rabbit IgG F(ab')₂(H+L)(AH); Ted Pella). Specimens were examined using a Tecnai G² Spirit BioTWIN transmission electron microscope operating at 80 kV. The images were obtained at magnifications of 23,000× to 49,000×.

Results

Colocalization of SYP-1, SYP-2, SYP-3, and SYP-4 at the interface between homologous chromosomes

Previous studies of SYP-1, SYP-2, SYP-3, and SYP-4 have demonstrated that all four proteins share a similar localization pattern throughout meiosis and are interdependent for this localization (MacQueen *et al.* 2002; Colaiacovo *et al.* 2003; Smolikov *et al.* 2007; Smolikov *et al.* 2009). The SYP proteins are first observed forming small foci and short patches on chromosomes at transition zone (leptotene/zygotene stages). By pachytene, these proteins localize continuously between homologous chromosomes. Co-immunostaining of wild-type gonads with pairwise combinations between SYP-1 and SYP-2, SYP-3, or SYP-4 antibodies reveals that all four proteins indeed colocalize at the interface between homologous chromosomes in pachytene nuclei when the SC is fully formed (Figure 1 and Smolikov *et al.* 2007).

An interaction between SYP-1 and SYP-2 is observed by co-immunoprecipitation

The interdependent colocalization of the SYP proteins at the interface between homologous chromosomes during meiosis suggests a potential interaction between these proteins. To investigate the association between the SYP-1 and SYP-2 proteins we performed immunoprecipitation (IP) experiments utilizing antibodies specific for either SYP-1 or SYP-2 and analyzed the precipitate for the presence of these two SYP proteins (a comparable analysis for SYP-3 and SYP-4 was not possible given that our antibodies do not detect these proteins on Western blots; see *Materials and Methods*). Western blot analysis of a wild-type precipitate using a SYP-1 antibody revealed a pull-down of both SYP-2 and SYP-1 (Figure 2, A and B, respectively). A similar result was obtained in converse co-immunoprecipitation experiments utilizing the SYP-2 antibody (Figure 2C). SYP-1 and SYP-2 were detected on IPs using wild-type lysates. Control IPs with lysates from either *syp-1* or *syp-2* null mutants that

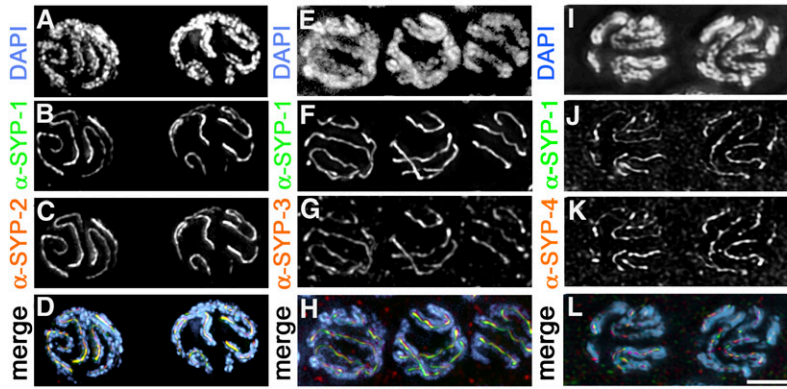


Figure 1 Colocalization of the SYP proteins at the interface between homologous chromosomes. High-magnification images of wild-type pachytene nuclei stained with DAPI (A, E, I in blue), α -SYP-1 (B, F, J in green), α -SYP-2 (C, red), α -SYP-3 (G, red), or α -SYP-4 (K, red). Scale bar, 2 μ m.

were treated with or without the antibody, and a wild-type lysate treated without any antibody, did not reveal similar results, hence supporting a specific interaction between the SYP-1 and SYP-2 proteins.

A yeast two-hybrid approach reveals the domains required for SYP-1 homotypic interactions and its interaction with SYP-2 and SYP-3

To further examine the protein–protein interactions involving the SC central region components, we analyzed the interactions between both full-length and truncated versions of SYP-1, SYP-2, and SYP-3 in a yeast two-hybrid interaction matrix (the analysis of the interactions between these SYP proteins and SYP-4 by this approach have been previously reported in Smolikov *et al.* 2009; see below).

Nine ORF-DNA-binding domain fusions consisting of the intact full-length, N-terminus deletion (Δ N) and C-terminus deletion (Δ C) for SYP-1, SYP-2, and SYP-3 were tested for yeast two-hybrid interactions with 156 AD fusions. The AD fusions consisted of full-length, Δ N, Δ C, and “domain-independent” deletions of all three SYP proteins. Moreover, these interactions were all tested in both directions by performing the reciprocal interaction matrix. As a result, a total of 936 interactions were tested. While the Δ N and Δ C constructs consist of deletions of defined regions of these proteins, such as the N-terminal or the C-terminal globular domains, the “domain-independent” deletions were generated by using all pairwise combinations of primers distributed 100 bp apart throughout the entire *syp-1*, *syp-2*, and *syp-3* cDNA sequences, regardless of the position of any specific domains, such as coiled-coil domains, present in the SYP proteins (see *Materials and Methods*). This strategy of combining full-length and domain-specific constructs along with what in essence is a “fragment library” has been recently shown to result in the rapid identification of regions involved in protein–protein interactions and to significantly increase the sensitivity of the yeast two-hybrid assay (Boxem *et al.* 2008).

Positive interactions were observed for only a subset of these constructs, as shown in Figure 3. Specifically, an interaction was observed between the full-length SYP-1, SYP-1 Δ C (1–402 aa), and SYP-1 Δ N (48–489 aa) constructs and the full-length SYP-1 as well as constructs consisting of the

N terminus plus the coiled-coil domain (1–420 aa) or just the coiled-coil domain of SYP-1 (36–418 aa), further supporting our previous results, which indicate that SYP-1 is capable of homotypic interactions. While the coiled-coil domain is sufficient for observing a homotypic interaction of SYP-1 when overexpressing these proteins from 2 μ plasmids (Figure 3, A–C), both the coiled-coil and the C-terminal domains of SYP-1 are required when expressing these proteins from centromeric plasmids (Figure S1).

Furthermore, an interaction was observed between SYP-1 and SYP-2 involving the coiled-coil region of SYP-1 and requiring the C-terminal region of SYP-2 (161–213 aa). These results further support the interactions detected by the IPs and reveal the domains that may be mediating such interactions.

Analysis of SYP-3 showed no homotypic interactions (data not shown). However, an interaction between SYP-3 and SYP-1 was revealed through the yeast two-hybrid approach utilizing the 2 μ plasmids (Figure 3, A–C). Specifically, interactions were observed between the full-length SYP-3 construct and full-length SYP-1, the construct carrying only the coiled-coil domain of SYP-1 (SYP-1cc) and the construct carrying both the N terminus and the coiled-coil domain of SYP-1 (SYP-1ncc). Moreover, the interaction between SYP-3 and SYP-1 requires both the N-terminal region of SYP-3 and the C-terminal region of SYP-1. However, the C-terminal region of SYP-1 alone is not sufficient for an interaction with SYP-3 (data not shown). Furthermore, while the loss of the N-terminal region of SYP-3 does not impede the interaction between full-length SYP-1 and SYP-3, the combined loss of the C-terminal region of SYP-1 and the N-terminal region of SYP-3 weakens the interaction ability. Assessment of a requirement for the C-terminal region of SYP-3 is hindered by the fact that this clone shows self-activation. Overall, the interactions observed between SYP-1 and SYP-3 were weaker than the homotypic interactions observed for SYP-1, for example, and only clearly apparent in the context of the 2 μ plasmid assay, further suggesting that a failure to detect the interaction between SYP-1 and SYP-3 through other methods might indeed stem from the either weaker or less stable nature of these interactions (Figure 3 and Figure S1).

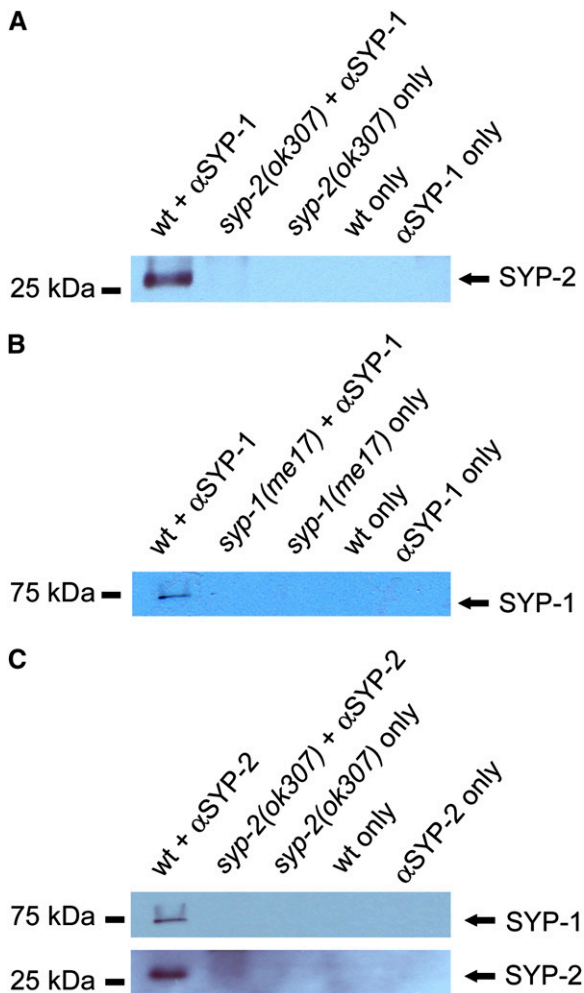


Figure 2 An interaction between SYP-1 and SYP-2 is observed by co-immunoprecipitation. Western blot analysis of co-immunoprecipitated proteins bound to SYP-1 (A and B) and SYP-2 (C) probed with α -SYP-1 and α -SYP-2 antibodies. As a control, co-immunoprecipitation was performed with the lysates of either *syp-1(me17)* or *syp-2(ok307)* null mutants. Furthermore, lysates of all genotypes underwent the same procedure without addition of the antibody (wt, *syp-2(ok307)*, and *syp-1(me17)* only) as well as a blank control (SYP-1 or SYP-2 only).

Finally, SYP-4 was identified as a SYP-3 interactor (Smolikov *et al.* 2009). Analysis of protein–protein interactions in a matrix utilizing full-length, N- and C-terminal truncations of all four SYP proteins revealed the interaction between SYP-3 and SYP-4 requires the N terminus of SYP-3 and the full length of SYP-4 and did not identify an interaction between SYP-4 and any of the other two SYP proteins (Smolikov *et al.* 2009).

Taken together, the findings presented in this study support a direct interaction between SYP-1 and both SYP-2 and SYP-3 and suggest that the interaction between SYP-1 and SYP-2 requires the coiled-coil domain of SYP-1 and the C terminus of SYP-2, whereas the interaction between SYP-1 and SYP-3 requires the C terminus of SYP-1 and the N terminus of SYP-3 (Figure 3D). Furthermore, the yeast two-hybrid analysis revealed that only SYP-1, but not SYP-2 or SYP-3, may be capable of homotypic interactions.

Immunoelectron microscopy analysis reveals the organization of the SYP proteins within the SC

The interdependent immunolocalization and protein–protein interactions observed for the SYP proteins provide further support to the notion that they act together in the central region of the SC. However, questions as to how these proteins are organized within this structure remain. Since immunostaining of whole-mounted gonads does not provide sufficient resolution for precisely determining the organization of SYP-1, SYP-2, SYP-3, and SYP-4 within the SC, we utilized immunoelectron microscopy instead. Therefore, we took advantage of antibodies raised against the N-terminal domains of SYP-1 and SYP-4 and the C-terminal domains of SYP-2 and SYP-3 (MacQueen *et al.* 2002; Colaiacovo *et al.* 2003; Smolikov *et al.* 2007, 2009) and performed immunogold labeling on ultrathin sections of wild-type gonads. Electron microscopic immunolocalization of the SYP proteins utilizing these primary antibodies, and secondary antibodies conjugated to either 10-nm or 15-nm gold particles, enabled us to examine the localization of the N or C termini of the SYP proteins with regard to the paired axes of the synapsed chromosomes in pachytene nuclei (Figure 4).

Interestingly, the gold particles corresponding to the anti-SYP-1-N antibody (69.84%; Figure 4A), the anti-SYP-2-C antibody (81.83%; Figure 4B) and the anti-SYP-4-N antibody (86.53%; Figure 4D) were located in the middle of the central region of the SC. In contrast, gold particles corresponding to the anti-SYP-3-C antibody (85.19%; Figure 4C) were located adjacent to the chromosome axes. This is the same region where gold particles corresponding to the anti-HTP-3 antibody, which recognizes a lateral element component of the SC (Goodyer *et al.* 2008), were detected (88%; Figure 4E; Figure S2).

To determine the exact distribution of gold particles with regard to the chromosome axes (defined by uranyl acetate staining), the shortest distance between each gold particle and the axis was measured (Δd ; Figure 4G) and compared to the overall distance between axes (*i.e.*, distance between the inner edge of the two chromosome axes) at that exact position (ΔD ; Figure 4G). Since the distance between the axes varies slightly for each SC sample (90 nm - 125 nm; average distance = 118 nm; Smolikov *et al.* 2008), the distance corresponding to the width of the SC (ΔD) was normalized to 100 and the distance from the gold particle to the axis (Δd) was recalculated, respectively (Figure 4G). This normalization of the distances allows for two things: first, it standardizes our measurements, which is required given the slight variations in SC width observed between sample preparations; second, it enables unspecific immunolabeling to be clearly identified, since the location of those gold particles will be observed at a lower frequency than the specific labeling. The normalization results in values between 0 and 50, with 0 corresponding to a localization adjacent to the chromatin, and 50 to a localization at the middle of the central region of the SC as shown in Figure 4G. The results for each analysis were pooled and divided into three regions of the SC:

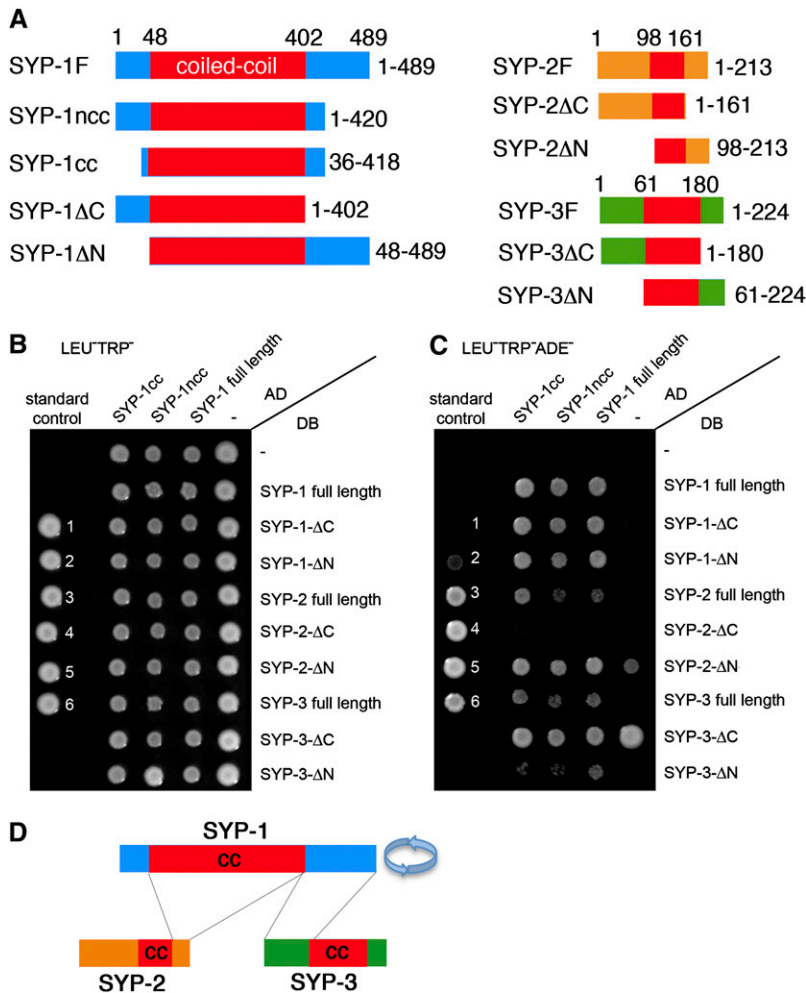


Figure 3 Yeast two-hybrid analysis reveals that SYP-1 interacts with both SYP-2 and SYP-3. The yeast two-hybrid system was applied to assess the interaction of truncated and full length SYP-1 (SYP-1cc, SYP-1ncc and SYP-1F, respectively) fused to the activation domain (AD) of GAL4, with full length SYP-1, SYP-2 and SYP-3 as well as N-terminal (Δ N) and C-terminal (Δ C) truncations for each fused to the DNA binding domain (DB) of GAL4. (A) Scheme of the various constructs utilized in this analysis. Globular domains are in blue, orange and green while coiled-coil domains are in red. Amino acid lengths are indicated. (B and C) Interactions were scored by growth on SC–Leu–Trp (B) and SC–Leu–Trp–Ade (C) plates. Negative (no. 1) and positive (nos. 2–6) controls are used as described in Walhout and Vidal (2001) and *Materials and Methods*. SYP-2 Δ N (DB) exhibited mild self-activation whereas SYP-3 Δ C (DB) exhibited strong self-activation and therefore its observed interactions are false positives. (D) Scheme of the interactions detected between SYP-1, SYP-2, and SYP-3. Lines interconnect the domains required for the interactions. Revolving arrows indicate self-interaction.

close proximity to the chromatin (0–10), a location midway between the chromosome axes and the middle of the central region (10–30), and a position in the middle of the central region (30–50). As expected, the lateral element component HTP-3 ($n = 25$), used as a control, was located adjacent to the chromatin and only a few gold particles could be seen in the middle of the central region of the SC (Figure 4, E and H, and Table S2). When the SC was probed with the anti-SYP-1-N, anti-SYP-2-C, or anti-SYP-4-N antibodies, the majority of gold particles ($n = 63$, $n = 44$, and $n = 51$, respectively) were located in the middle of the central region of the SC. Specifically, 65.08% of the gold particles corresponding to SYP-1-N were found in the region between 30 and 50, and 46% of all gold particles localized in the region between 40 and 50 (Figure 4H, Tables S2 and S3). In the case of SYP-2-C, 70.45% of all gold particles detected were located in the region between 30 and 50 and 54.55% in the region between 40 and 50 (Figure 4H, Table S2, and Table S3). Finally, in the case of SYP-4-N, 66.67% of all gold particles were located in the region between 30 and 50 and 37.25% between 40 and 50. In contrast, 85.19% of gold particles corresponding to SYP-3-C were found in proximity to the chromosome axes and 74.1% directly adjacent to the chromatin (Figure 4H and Table S2).

Narrowing down the intervals comprising the middle of the central region of the SC (30–40 and 40–50) did not reveal a difference between the localization of SYP-1, SYP-2, and SYP-4 suggesting that the N-terminal domain of SYP-1, the C-terminal domain of SYP-2, and the N-terminal domain of SYP-4 are in close proximity to each other. The proximity between the SYP-1 and SYP-2 domains is further supported by our double labeling experiments where gold particles corresponding to SYP-1 and to SYP-2 could be found colocalizing at the center of the SC (Figure 4F).

This is the first time that the position of the SYP proteins both within the SC and with regard to each other is demonstrated in *C. elegans* meiotic nuclei at an ultrastructural level. This analysis suggests that the C-terminal domain of SYP-3 is found adjacent to the chromatin, whereas the N-terminal domain of SYP-1, the C-terminal domain of SYP-2, and the N-terminal domain of SYP-4 are located close to each other at the middle of the central region of the SC.

Discussion

Organization of the SC

The analyses of the SCs in different organisms reveal that its general structure is highly conserved. The degree of

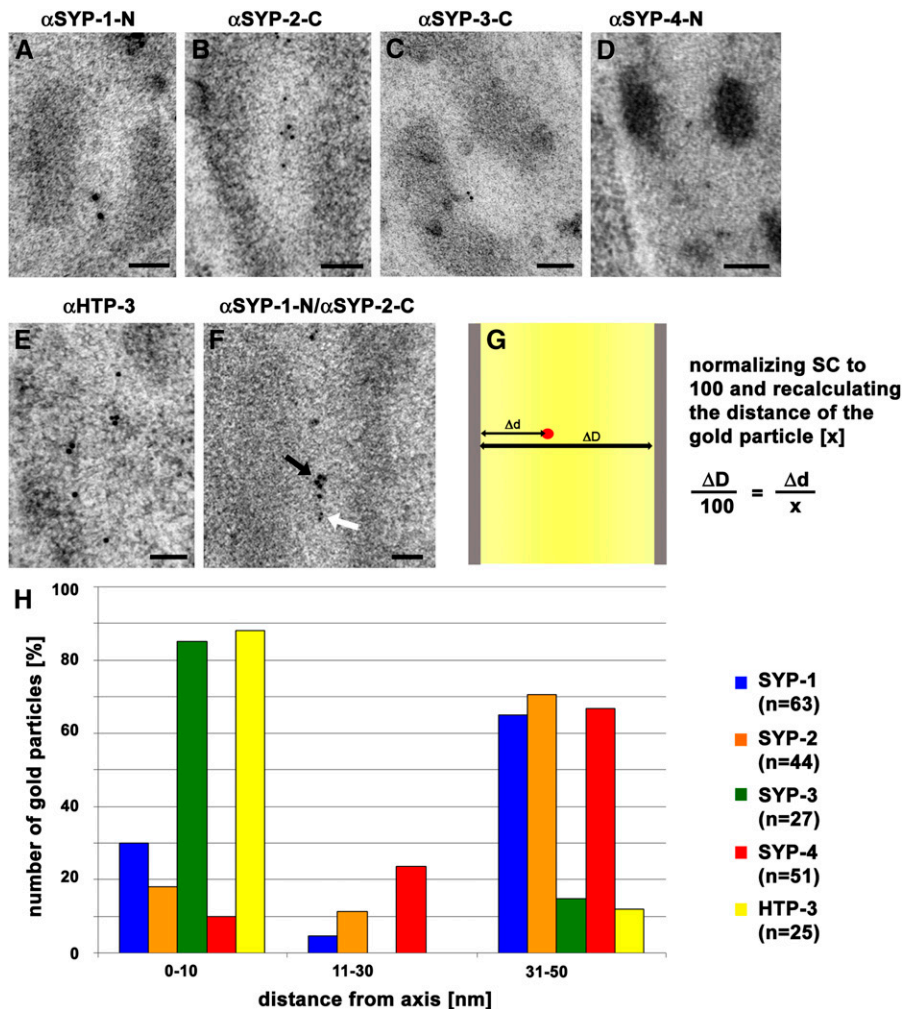


Figure 4 Ultrastructural localization of SYP-1, SYP-2, SYP-3, and SYP-4 on the central region of the SC by immunoelectron microscopy. Immunogold labeling of the N terminus of SYP-1 (A), C terminus of SYP-2 (B), C terminus of SYP-3 (C), N terminus of SYP-4 (D), HTP-3 (E), and a double labeling for SYP-1-N (15-nm gold, black arrow) and SYP-2-C (10-nm gold, white arrow) (F) on wild-type SCs from pachytene nuclei. Gray: chromatin; black dots: gold particles (coupled to secondary antibody). (G) Distribution of gold particles on the SC. The width of the SC (ΔD , distance between chromosome axes) was measured through each gold particle and normalized to 100. The shortest distance between the gold particle and a chromosome axis (Δd) was measured and recalculated accordingly. Gray: axes, red: gold particle. (H) Graph depicting the quantitation of the number of gold particles (%) found throughout three sectors of the SC, where 0 nm represents the axis, whereas 50 nm represents the middle of the SC.

organization of the SC seems to vary slightly among species with mammals having a lesser degree of organization than either yeast or insects (Schmekel *et al.* 1993a). However, the organization of the transverse filaments in yeast, *Drosophila*, and mammals is similar. Specifically, these transverse filaments homodimerize in a head-to-tail organization with their C termini anchored to the chromosomes and their N termini located in the center of the SC (Sym and Roeder 1995; Liu *et al.* 1996; Schmekel *et al.* 1996; Dong and Roeder 2000; Anderson *et al.* 2005; Öllinger *et al.* 2005). The N-terminal portions of the transverse filaments have been proposed to overlap, allowing the proteins to form polydimers. Deletion of the N terminus has been shown to block this interaction. Specifically, the deletion of a small portion of the coiled-coil region adjacent to the N terminus of the *Drosophila* C(3)G protein results in a lack of formation of anti-parallel pairs of C(3)G homodimers (tetramers), further supporting the relevance of the N-terminal overlap (Jeffress *et al.* 2007).

In addition to the transverse filament proteins, other proteins such as SYCE1, SYCE2, SYCE3, and TEX12 in mouse and CONA in *Drosophila* localize to the central region of the SC and have been proposed to form the central element of

this structure (Costa *et al.* 2005; Hamer *et al.* 2006; Bolcun-Filas *et al.* 2007; Page *et al.* 2008; Schramm *et al.* 2011; Lake and Hawley, personal communication). Interestingly, electron microscopic analysis of mouse testis sections failed to detect a central element (Bolcun-Filas *et al.* 2009). This is most likely due to the nature of the two-dimensional analysis performed when in fact the SC is a three-dimensional structure with thickness since it is composed of “stacked” or multilayered transverse filaments and central element proteins (Schmekel *et al.* 1993a,b). In addition, the central element is less ordered and its proteins apparently less frequent in mammals, compared to the beetle *Blaps cribrosa* and *D. melanogaster*, making its detection less facile (Schmekel *et al.* 1993a). Interestingly, a central element is also not apparent by electron microscopic analysis of thin sections of pachytene nuclei in *C. elegans*; however, this is the only other model system in which multiple central region components have been identified thus far (MacQueen *et al.* 2002; Colaiacovo *et al.* 2003; Smolikov *et al.* 2007, 2009). Our analysis of their binding abilities and their localization within the SC lead us to propose a model for how the SYP proteins are organized with regard to each other and to the chromatin axes ultimately forming the SC of *C. elegans* (Figure 5).

We have shown above that *SYP-1*, a 490-amino-acid protein, undergoes homotypic interactions. The coiled-coil domain of *SYP-1* is important for this interaction, as determined by the yeast two-hybrid approach. Furthermore, 65% of the gold particles specific for the N terminus of *SYP-1* were found localized at the center of the SC. This suggests that the self-interacting units of *SYP-1* are most likely arranged in a parallel orientation with their N termini positioned toward the middle of the SC. If *SYP-1* would self-interact in an anti-parallel fashion, one would predict that the localization of the gold particles would be more widespread (heterogeneous) and in closer proximity to the axes. Therefore our findings suggest a similar homotypic organization for *SYP-1* as proposed for yeast Zip1 (Dong and Roeder 2000), fly C(3)G (Anderson *et al.* 2005), and mouse SCP1 (Liu *et al.* 1996).

Homotypic interactions were not detected for the small *SYP-2* protein (213 amino acids), which carries a coiled-coil domain flanked by globular domains (Colaiacovo *et al.* 2003). Its C-terminal domain, however, is necessary for its interaction with *SYP-1*, as revealed by the yeast two-hybrid studies, and further supporting the *SYP-1/SYP-2* interaction detected both by expression in *Xenopus* XTC cells, a heterologous system where meiotic proteins are not normally expressed (data not shown), and by co-immunoprecipitation. Furthermore, immuno-gold localization revealed that gold particles corresponding to the C-terminal end of *SYP-2* were localized at the center of the SC. Their localization is in close proximity to the gold particles identifying the N-terminal end of *SYP-1* (Figure 4F). One possible configuration that can accommodate these observations places the C-terminal domain of *SYP-2* both near the center of the SC and near the N-terminal domain of *SYP-1* (Figure 5), since the distances measured between gold α -*SYP-1*/ gold α -*SYP-2* did not reveal any significant variations (Table S2, Table S3,

and Table S4). However, we cannot rule out that the small *SYP-2* protein is folded and arranged in an opposite direction at the same position.

SYP-3 is a 225-amino-acid protein. Immunogold labeling places the C terminus of the *SYP-3* protein at or near the chromosome axes. An interaction between *SYP-3* and *SYP-1* was detected by the yeast two-hybrid approach when utilizing the overexpression plasmid system. This analysis revealed that the interaction involves the N terminus of *SYP-3* and the C terminus of *SYP-1*. Moreover, utilizing a yeast two-hybrid approach, we recently identified *SYP-4* as a *SYP-3* interactor in *C. elegans* and this interaction involves the N terminus of *SYP-3* (Smolikov *et al.* 2009).

The recently identified *SYP-4* protein is the largest of the SYP proteins (605 amino acids). Immunolocalization of the protein via electron microscopy places its N-terminal end toward the center of the SC (Figure 4D; Figure 5). The localization of *SYP-4*, in close proximity to *SYP-1* and *SYP-2*, as well as its size and its interaction with *SYP-3*, complete the framework of interactions between the various SYP proteins.

Connecting the lateral elements

Our findings provide the first insights into the localization/organization of all four known SYP proteins within the SC, as well as some of their binding abilities. Several interesting features about the organization of the SC were revealed through this study. Specifically, the two small SYP proteins (*SYP-2* and *SYP-3*) are separated from each other within the SC structure given their positions and sizes. The small *SYP-2* protein was localized at the center of the SC while *SYP-3* was localized at the axes. However, both small proteins share in common that they interact with larger SYP proteins. Furthermore, the N termini of the larger *SYP-1* and *SYP-4* proteins both localize to the center of the SC. While a *SYP-1*

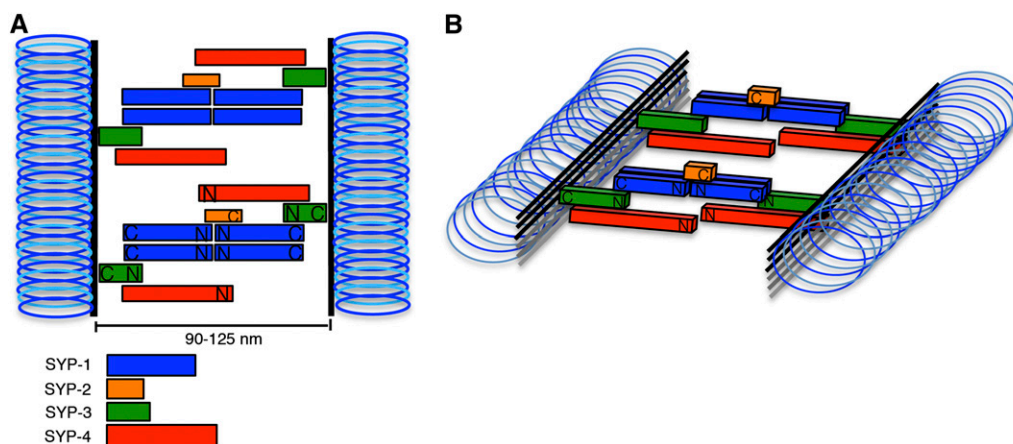


Figure 5 Model for the organization of the SYP proteins in the central region of the SC in *C. elegans*. SC structure. (A) Scheme of the position and organization of the SYP proteins in the SC portrayed on a single plane. *SYP-1* (blue) is oriented in the SC reaching with its N-terminus domain into the middle of the central region. Homodimerization (or higher-order assembly) of *SYP-1* presumably occurs in a parallel fashion although head-to-head polymerization cannot be ruled out. *SYP-2* (orange) is localized with its C terminus at the center

of the central region of the SC and interacts with *SYP-1*. Alignment to *SYP-1* is depicted as antiparallel since this is the shortest possible distance between the *SYP-1*-N terminus and the *SYP-2* C terminus (other orientation cannot be ruled out). *SYP-3* (green), which interacts with *SYP-4* and weakly with *SYP-1*, but not *SYP-2*, localizes with its C-terminal domain at the chromosome axis. *SYP-4* (red), which associates with *SYP-3*, localizes with its N terminus at the center of the central region of the SC. Range of distances measured between homologous axes by EM in pachytene stage nuclei is depicted. Chromatin loops (blue); lateral elements (black vertical lines). (B) Scheme of a cross-section of the SC demonstrating how the organization of the SYP proteins may contribute not only to the width but also to the thickness of this structure.

homodimer may be able to span over a quarter of the SC width just with its coiled-coil domain of 34.16 nm, *SYP-4* seems to span the distance from the center of the SC to the coiled-coil domain of *SYP-3*. Therefore, from a theoretical point of view, the four SYP proteins have the potential to connect both axes of the SC.

We also detected the ability of individually expressed GFP-tagged *SYP-1*, but not *SYP-2*, to form aggregates in XTC cells, which most likely correspond to the higher-order protein structures referred to as polycomplexes (data not shown). Although we have no indication that *SYP-4* or *SYP-3* would be capable of homotypic interactions, the results of the heterologous system suggest that at least *SYP-1* has this ability. Both N- and C-terminus GFP-tagged *SYP-1* proteins were able to form aggregates independent of other meiotic proteins in the heterologous system. This ability is similar to that observed for either SYCP-1 (Öllinger *et al.* 2005) or Zip1 (Sym and Roeder 1995), supporting the capacity of *SYP-1* to form polycomplexes. Furthermore, the yeast two-hybrid data revealed that only the C terminus, but not the N terminus, of *SYP-1* is necessary for *SYP-1* self-interaction. We cannot rule out the possibility that limitations of the yeast two-hybrid system precludes the detection of a possible head-to-head interaction of two *SYP-1* proteins. This, presumably weak interaction might be stabilized by its identified binding partner, *SYP-2*.

SYP-1 and *SYP-2*, therefore, would form a module that is connected to a second module of interacting proteins, namely *SYP-4* and *SYP-3* that would link to the lateral elements.

The width of the SC

Previous measurements of the width of the SC in pachytene nuclei in wild-type *C. elegans* identified a range between 90 and 125 nm with the average width being 118 nm (Smolikov *et al.* 2008). This is comparable to the widths of SCs throughout other species (Goldstein 1987; Sym *et al.* 1993; Zickler and Kleckner 1999; Page and Hawley 2003).

It has been proposed that the width of the SC is highly dependent on the size of the coiled-coil domain of the connecting transverse filaments (Sym and Roeder 1995; Tung and Roeder 1998; Öllinger *et al.* 2005; Anderson *et al.* 2005). The lengths for most transverse filaments have been predicted to be approximately 70–90 nm (Hunter 2003) allowing some room for a head-to-head interaction between the proteins (Liu *et al.* 1996; Schmekel *et al.* 1996). In contrast, the predicted size of the coiled-coil domain for *SYP-1* (harboring the largest coiled-coil domain among all the SYP-proteins) is relatively short, being only 34.16 nm. Even a head-to-head polymerization would not be able to span the 100 nm of the SC. However, considering the coiled-coil domains of *SYP-2*, *-3*, and *-4* (5.05, 13.51, and 12.92 nm, respectively; Smolikov *et al.* 2009), and the fact that we are dealing with a three-dimensional structure, the potential to span the given distance is within reach.

Altogether our data suggest a similar organization of the SC in *C. elegans* to that proposed for this structure in rats

and mice, namely, a role for some of its components in determining width while others may play a primary role in determining thickness, as well as a less-defined central element. Taken together, this study better delineates the platform upon which various other critical meiotic events take place, revealing both the similarities and distinct features of the *C. elegans* SC compared to other organisms.

Acknowledgments

We thank Scott Hawley for critical reading of this manuscript and Monique Zetka for the HTP-3 antibody. K.S.-P. was supported by a Deutsche Forschungsgemeinschaft German Research Foundation postdoctoral research fellowship (PR1057/1-1). This work was supported by research grant 5-FY05-1214 from the March of Dimes Birth Defects Foundation and by National Institutes of Health grant R01GM072551 to M.P.C.

Literature Cited

- Anderson, L. K., S. M. Royer, S. L. Page, K. S. McKim, A. Lai *et al.*, 2005 Juxtaposition of C(2)M and the transverse filament protein C(3)G within the central region of Drosophila synaptonemal complex. *Proc. Natl. Acad. Sci. USA* 102: 4482–4487.
- Bolcun-Filas, E., Y. Costa, R. Speed, M. Taggart, R. Benavente *et al.*, 2007 SYCE2 is required for synaptonemal complex assembly, double strand break repair, and homologous recombination. *J. Cell Biol.* 176: 741–747.
- Bolcun-Filas, E., E. Hall, R. Speed, M. Taggart, C. Grey *et al.*, 2009 Mutation of the mouse Syce1 gene disrupts synapsis and suggests a link between synaptonemal complex structural components and DNA repair. *PLoS Genet.* 5: e1000393.
- Boxem, M., Z. Maliga, N. Klitgord, N. Li, I. Lemmens *et al.*, 2008 A protein domain-based interactome network for *C. elegans* early embryogenesis. *Cell* 134: 534–545.
- Brenner, S., 1974 The genetics of *Caenorhabditis elegans*. *Genetics* 77: 71–94.
- Colaiacovo, M. P., A. J. MacQueen, E. Martinez-Perez, K. McDonald, A. Adamo *et al.*, 2003 Synaptonemal complex assembly in *C. elegans* is dispensable for loading strand-exchange proteins but critical for proper completion of recombination. *Dev. Cell* 5: 463–474.
- Costa, Y., R. Speed, R. Ollinger, M. Alsheimer, C. A. Semple *et al.*, 2005 Two novel proteins recruited by synaptonemal complex protein 1 (SYCP1) are at the centre of meiosis. *J. Cell Sci.* 118: 2755–2762.
- Dong, H., and G. S. Roeder, 2000 Organization of the yeast Zip1 protein within the central region of the synaptonemal complex. *J. Cell Biol.* 148: 417–426.
- Goodyer, W., S. Kaitna, F. Couteau, J. D. Ward, S. J. Boulton *et al.*, 2008 HTP-3 links DSB formation with homolog pairing and crossing over during *C. elegans* meiosis. *Dev. Cell* 14: 263–274.
- Goldstein, P., 1987 Multiple synaptonemal complexes (polycomplexes): origin, structure and function. *Cell Biol. Int. Rep.* 11: 759–796.
- Hamer, G., K. Gell, A. Krouznetsova, I. Novak, R. Benavente *et al.*, 2006 Characterization of a novel meiosis-specific protein within the central element of the synaptonemal complex. *J. Cell Sci.* 119: 4025–4032.
- Higgins, J. D., E. Sanchez-Moran, S. J. Armstrong, G. H. Jones, and F. C. Franklin, 2005 The Arabidopsis synaptonemal complex

- protein ZYP1 is required for chromosome synapsis and normal fidelity of crossing over. *Genes Dev.* 19: 2488–2500.
- Hunter, N., 2003 Synaptonemal complexities and commonalities. *Mol. Cell* 12: 533–539.
- Jeffress, J. K., S. L. Page, S. K. Royer, E. D. Belden, J. P. Blumenstiel *et al.*, 2007 The formation of the central element of the synaptonemal complex may occur by multiple mechanisms: the roles of the N- and C-terminal domains of the *Drosophila* C(3)G protein in mediating synapsis and recombination. *Genetics* 177: 2445–2456.
- Laemmli, U. K., 1970 Cleavage of structural proteins during the assembly of the head of bacteriophage T4. *Nature* 227: 680–685.
- Liu, J. G., L. Yuan, E. Brundell, B. Björkroth, B. Daneholt *et al.*, 1996 Localization of the N-terminus of SCP1 to the central element of the synaptonemal complex and evidence for direct interactions between the N-termini of SCP1 molecules organized head-to-head. *Exp. Cell Res.* 226: 11–19.
- MacQueen, A. J., M. P. Colaiacovo, K. McDonald, and A. M. Villeneuve, 2002 Synapsis-dependent and -independent mechanisms stabilize homolog pairing during meiotic prophase in *C. elegans*. *Genes Dev.* 16: 2428–2442.
- McDonald, K., 1998 High pressure freezing for preservation of high resolution fine structure and antigenicity for immunolabeling. *Methods Mol. Biol.* 117: 77–97.
- Meuwissen, R. L., H. H. Offenberg, A. J. Dietrich, A. Riesewijk, M. Van Iersel *et al.*, 1992 A coiled-coil related protein specific for synapsed regions of meiotic prophase chromosomes. *EMBO J.* 11: 5091–5100.
- Öllinger, R., M. Alsheimer, and R. Benavente, 2005 Mammalian protein SCP1 forms synaptonemal complex-like structures in the absence of meiotic chromosomes. *Mol. Biol. Cell* 16: 212–217.
- Osman, K., E. Sanchez-Moran, J. D. Higgins, G. H. Jones, and F. C. Franklin, 2006 Chromosome synapsis in *Arabidopsis*: analysis of the transverse filament protein ZYP1 reveals novel functions for the synaptonemal complex. *Chromosoma* 115: 212–219.
- Page, S. L., and R. S. Hawley, 2001 (3)G encodes a *Drosophila* synaptonemal complex protein. *Genes Dev.* 15: 3130–3143.
- Page, S. L., and R. S. Hawley, 2003 Chromosome choreography: the meiotic ballet. *Science* 301: 785–789.
- Page, S. L., and R. S. Hawley, 2004 The genetics and molecular biology of the synaptonemal complex. *Annu. Rev. Cell Dev. Biol.* 20: 525–558.
- Page, S. L., R. S. Khetani, C. M. Lake, R. J. Nielsen, J. K. Jeffress *et al.*, 2008 Corona is required for higher-order assembly of transverse filaments into full-length synaptonemal complex in *Drosophila* oocytes. *PLoS Genet.* 4: e1000194.
- Schmekel, K., U. Skoglund, and B. Daneholt, 1993a The three-dimensional structure of the central region in a synaptonemal complex: a comparison between rat and two insect species, *Drosophila melanogaster* and *Blaps cribrosa*. *Chromosoma* 102: 682–692.
- Schmekel, K., J. Wahrman, U. Skoglund, and B. Daneholt, 1993b The central region of the synaptonemal complex in *Blaps cribrosa* studied by electron microscope tomography. *Chromosoma* 102: 669–681.
- Schmekel, K., R. L. Meuwissen, A. J. Dietrich, A. C. Vink, J. Van Marle *et al.*, 1996 Organization of SCP1 protein molecules within synaptonemal complexes of the rat. *Exp. Cell Res.* 226: 20–30.
- Schramm, S., J. Fraune, R. Naumann, A. Hernandez-Hernandez, C. Höög *et al.*, 2011 A novel mouse synaptonemal complex protein is essential for loading of central element proteins, recombination, and fertility. *PLoS Genet.* 7(5): e1002088.
- Smolikov, S., A. Eizinger, A. Hurlburt, E. Rogers, A. M. Villeneuve *et al.*, 2007 Synapsis-defective mutants reveal a correlation between chromosome conformation and the mode of double-strand break repair during *Caenorhabditis elegans* meiosis. *Genetics* 176: 2027–2033.
- Smolikov, S., K. Schild-Prüfert, and M. P. Colaiacovo, 2008 CRA-1 uncovers a double-strand break-dependent pathway promoting the assembly of central region proteins on chromosome axes during *C. elegans* meiosis. *PLoS Genet.* 4(6): e1000088.
- Smolikov, S., K. Schild-Prüfert, and M. P. Colaiacovo, 2009 A yeast two-hybrid screen for SYP-3 interactors identifies SYP-4, a component required for synaptonemal complex assembly and chiasma formation in *Caenorhabditis elegans* meiosis. *PLoS Genet.* 5: e1000669.
- Sym, M., and G. S. Roeder, 1995 Zip1-induced changes in synaptonemal complex structure and polycomplex assembly. *J. Cell Biol.* 128: 455–466.
- Sym, M., J. A. Engebrecht, and G. S. Roeder, 1993 ZIP1 is a synaptonemal complex protein required for meiotic chromosome synapsis. *Cell* 72: 365–378.
- Tung, K. S., and G. S. Roeder, 1998 Meiotic chromosome morphology and behavior in zip1 mutants of *Saccharomyces cerevisiae*. *Genetics* 149: 817–832.
- Vidal, M., R. K. Brachmann, A. Fattaey, E. Harlow, and J. D. Boeke, 1996 Reverse two-hybrid and one-hybrid systems to detect dissociation of protein-protein and DNA-protein interactions. *Proc. Natl. Acad. Sci. USA* 93: 10315–10320.
- Walhout, A. J., and M. Vidal, 2001 High-throughput yeast two-hybrid assays for large-scale protein interaction mapping. *Methods* 24: 297–306.
- Zickler, D., and N. Kleckner, 1999 Meiotic chromosomes: integrating structure and function. *Annu. Rev. Genet.* 33: 603–754.

Communicating editor: G. P. Copenhaver

GENETICS

Supporting Information

<http://www.genetics.org/content/suppl/2011/08/12/genetics.111.132431.DC1>

Organization of the Synaptonemal Complex During Meiosis in *Caenorhabditis elegans*

Kristina Schild-Prüfert, Takamune T. Saito, Sarit Smolikov, Yanjie Gu, Marina Hincapie,
David E. Hill, Marc Vidal, Kent McDonald, and Monica P. Colaiácovo

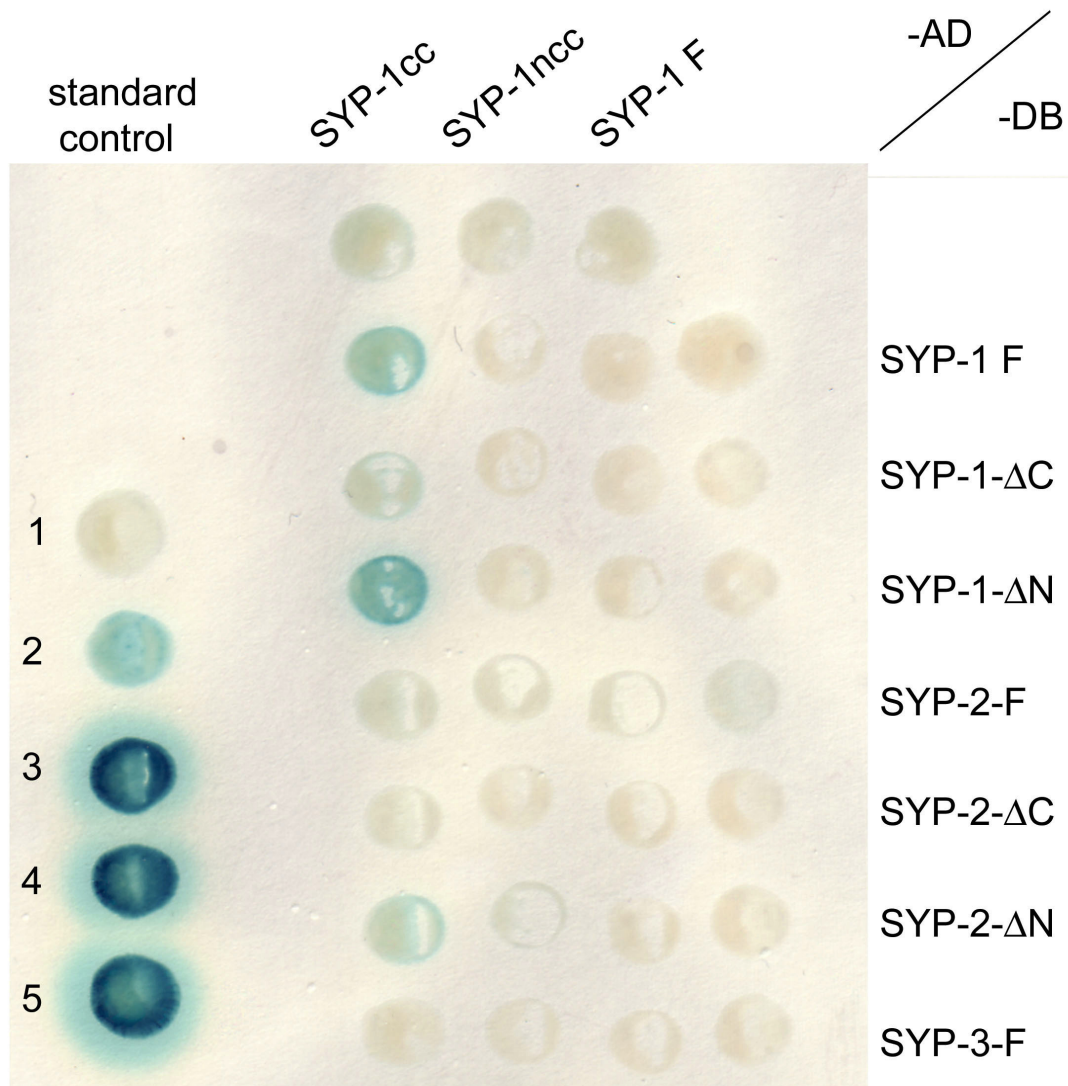


Figure S1 Yeast two-hybrid assay reveals interaction between SYP-1 and SYP-2 proteins. The yeast two-hybrid approach was used to test for protein interactions between truncated and full length SYP-1 fused to the activation domain (AD) of GAL4, and full length SYP-1, SYP-2 and SYP-3, as well as N-terminal (Δ N) and C-terminal (Δ C) truncations for SYP-1 and SYP-2, fused to the DNA binding domain (DB) of GAL4. Constructs and fragment sizes are depicted in Figure 4. Positive interactions were assessed by β -galactosidase activity. Numbers 1 to 5 represent standard controls as described in (WALHOUT and VIDAL 2001) and Materials and Methods.

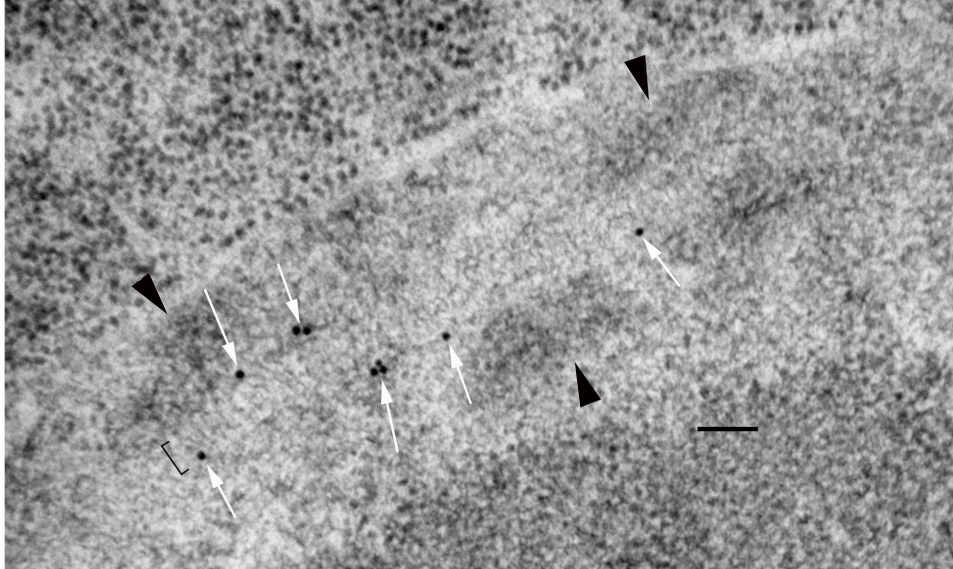


Figure S2 Ultrastructural localization of HTP-3 by immuno-EM analysis of wild type SCs. Transmission electron micrograph of an SC in a pachytene nucleus from a wild type germline, labeled with a primary antibody against HTP-3 visualized with a gold-conjugated secondary antibody (indicated by white arrows). Electron-dense chromatin patches (indicated by arrowheads) are arranged in parallel; ladder-like structure formed by transverse filaments is clearly evident at this magnification (indicated by black bracket). This image depicts the same SC shown at a higher magnification in Figure 4, but allows for a better appreciation of the zipper-like organization of this structure. Scale bar, 100nm.

Table S1 Primers used for cloning full length (F) and truncated *syp-1*, *syp-2* and *syp-3* into the Gateway entry vector (pDONR223).

Fragment	Primer Pairs
SYP-1-F	SYP-1F-5'(GGGGACAACCTTTGTACAAAAAAGTTGGCCATGGATAACTTCACAATTTGGGT) SYP-1F-3'(GGGGACAACCTTTGTACAAGAAAGTTGGGTATTTCTCCCTCCTCTCTTT)
SYP-1-ΔC	SYP-1ΔC-5'(GGGGACAACCTTTGTACAAAAAAGTTGGCCATGGATAACTTCACAATTTGGGT) SYP-1ΔC-3'(GGGGACAACCTTTGTACAAGAAAGTTGGAGCACGTTGTTCTTTAATTTGATT)
SYP-1-ΔN	SYP-1ΔN-5'(GGGGACAACCTTTGTACAAAAAAGTTGGCCGAGCAAGATAAAGGCGAGCA) SYP-1ΔN-3'(GGGGACAACCTTTGTACAAGAAAGTTGGGTATTTCTCCCTCCTCTCTTT)
SYP-1-cc	SYP-1-cc-5'(GGGGACAACCTTTGTACAAAAAAGTTGGCCAGCAATACGTTCTTGAGAAGC) SYP-1-cc-3'(GGGGACAACCTTTGTACAAGAAAGTTGGGTAAGTGGTGTGCTCGT)
SYP-1-ncc	SYP-1-ncc-5'(GGGGACAACCTTTGTACAAAAAAGTTGGCCATGGATAACTTCACAATTTGGGT) SYP-1-ncc-3'(GGGGACAACCTTTGTACAAGAAAGTTGGGTAAGTGGTGTGCTCGT)
SYP-2-F	SYP-2F-5'(GGGGACAACCTTTGTACAAAAAAGTTGGCCATGAATTCTGCCATCGATCT) SYP-2F-3'(GGGGACAACCTTTGTACAAGAAAGTTGGGTATAACTTGTGAGCCAC)
SYP-2-ΔC	SYP-2ΔC-5'(GGGGACAACCTTTGTACAAAAAAGTTGGCCATGAATTCTGCCATCGATCT) SYP-2ΔC-3'(GGGGACAACCTTTGTACAAGAAAGTTGGTCTGGCGTCAACGCGATTT)
SYP-2-ΔN	SYP-2ΔN-5'(GGGGACAACCTTTGTACAAAAAAGTTGGCCACACAAGATCTGACAATGGAGCTGG) SYP-2ΔN-3'(GGGGACAACCTTTGTACAAGAAAGTTGGGTATAACTTGTGAGCCAC)
SYP-3-F	SYP-3F-5'(GGGACAACCTTTGTACAAAAAAGTTGGCATGAATTCGAAAAGCTTGT) SYP-3F-3'(GGGGACAACCTTTGTACAAGAAAGTTGGTCATGTAGAAAAGTCGGGCT)
SYP-3-ΔC	SYP-3ΔC-5'(GGGACAACCTTTGTACAAAAAAGTTGGCATGAATTCGAAAAGCTTGT) SYP-3ΔC-3'(GGGGACAACCTTTGTACAAGAAAGTTGGACGGAGAGAAGGAATCATTCA)
SYP-3-ΔN	SYP-3ΔN-5'(GGGGACAACCTTTGTACAAAAAAGTTGGCGAAGACAGGGTAAATGTGCTGCTCAA) SYP-3ΔN-3'(GGGGACAACCTTTGTACAAGAAAGTTGGTCATGTAGAAAAGTCGGGCT)

Table S2 Percentage of gold particles found in a normalized SC divided into 3 sections: in the proximity of the axes (0-10), midway between the axes and the middle of the central region of the SC (11-30), and in the middle of the central region of the SC (31-50).

Primary Antibody	0-10	11-30	31-50
SYP-1-N (n= 63)	30.2 %	4.8 %	65 %
SYP-2-C (n= 44)	18.2 %	11.4 %	70.4 %
SYP-3-C (n= 27)	85.2 %	0 %	14.8 %
SYP-4-N (n= 51)	9.8%	23.5 %	66.7 %
HTP-3 (n= 25)	88 %	0 %	12 %

Table S3 Percentage of gold particles found in a normalized SC divided into 5 equal sections: in the proximity of the axes (0-10), between the axes and the middle of the central region of the SC (11- 20), (21-30), and at the center of the SC (31-40), (41-50).

Primary Antibody	0-10	11-20	21-30	31-40	41-50
SYP-1-N (n= 63)	30.2 %	0 %	4.8 %	19 %	46 %
SYP-2-C (n= 44)	18.2 %	4.5 %	6.8 %	16 %	54.5 %
SYP-3-C (n= 27)	85.2 %	0 %	0 %	3.7 %	11.1%
SYP-4-N (n= 51)	9.8 %	2 %	21.6 %	29.4 %	37.2%
HTP-3 (n= 25)	88 %	0 %	0 %	4 %	8 %

Table S4 Normalized distances ($\chi = \Delta d^{*100} / \Delta d$) of gold particles found in wild type SCs. Distances are indicated in nm.

SYP1-N (n= 63)	SYP2-C (n= 44)	SYP3-C (n=27)	SYP4-N (n=51)	HTP3 (n=25)
0	0	0	0	0
0	0	0	0	0
0	0	0	0	0
0	0	0	0	0
0	0	0	4.78	0
0	0	0	11.07	0
0	0	0	21.25	0
0	0	0	24.9	0
0	14.31	0	26.8	0
0	17.56	0	27.12	0
0	21.41	0	27.6	0
0	21.77	0	27.7	0
0	28.33	0	28.22	0
0	31.02	0	28.99	0
0	32.86	0	29.08	0
0	33.3	0	29.75	0
0	34.17	0	30.32	0
0	37.06	0	31.8	0
0	37.46	0	32.4	0
20.97	39.75	0	32.82	0
26.01	41.09	0	33.08	1.74
27.04	42.8	0.99	33.27	4.2
31.61	42.93	1.2	33.5	36.42
32.12	43.5	38.67	33.98	43.59
32.86	43.66	40.57	34.01	44.18
33.76	43.7	42.45	36	
35.21	43.81	47.36	37.3	
36.67	44.3		37.64	
36.85	44.41		37.88	
37.86	44.68		38	
38.26	44.86		39.58	
38.69	45.04		39.76	
39.06	45.77		40.42	
39.8	46.25		40.65	
40.71	46.9		40.71	
41.57	47.06		41.75	

41.62	47.42	42
41.89	47.72	42
42.29	48.21	42.02
43.54	48.73	42.02
44.04	48.73	42.32
44.42	49.62	42.97
44.65	49.72	44.07
44.74	49.82	44.8
44.86		44.92
45.35		45.28
45.51		45.98
45.55		46
45.67		48.04
45.95		49.42
46.43		49.5
46.54		
46.96		
47.8		
47.9		
48		
48.22		
48.42		
49.34		
49.42		
49.68		
49.74		
50		
